Heat transfer on a naturally cross-driven ventilated triangular cavity with openings

2009 J. Phys.: Conf. Ser. 166 012019

(http://iopscience.iop.org/1742-6596/166/1/012019)

Journal of Physics: Conference Series **166** (2009) 012019 doi:10.1088/1742-6596/166/1/012019

Heat transfer on a naturally cross-driven ventilated triangular cavity with openings.

M E Berli[1, 2], J Di Paolo[2] and F A Saita[1]
[1] INTEC, Universidad Nacional del Litoral, Güemes 3450, 3000, Santa Fe, Argentina.
[2] GIMEF, Departamento Ingeniería Industrial, FRSF - UTN, Lavaise 610, 3000, Santa Fe, Argentina

E-mail: mberli@santafe-conicet.gov.ar

Abstract. This work addresses the problem of heat transfer through the roof of a family home with the purpose of improving air-conditioning energy savings during hot summer days. To this end, the air natural convection in a right-angle triangular cavity, resembling an attic, is numerically analyzed. The air cavity is assumed as naturally ventilated through two openings that induce an external air-stream flowing into and out of the cavity. The governing equations for both flow and heat transfer are simultaneously solved with appropriate boundary conditions. Finite element technique is employed to transform the original set of differential equations into a non-linear discrete one, which is finally solved by Newton iteration. Two major assumptions are made, namely: radiation heat transfer is negligible and the air flow is in laminar regime; in addition, the usual Boussinesq approximation is employed. Under these assumptions the numerical predictions show that the amount of heat transferred through the ceiling rapidly diminishes as the flow through the cavity increases. Therefore; whether or not the ceiling is insulated, the energy transfer is reduced by more than 50% and energy savings are considerably improved.

1. Introduction

The roof of a family home is usually the component that transfers more heat than any other wall of the house. The large temperature gradient that exists between the roof and the ceiling on days of extremely hot temperatures, introduces important amounts of energy that needs to be eliminated to keep the interior comfortable. In this sense, an air cavity located between the roof and the ceiling might produce important energy savings if it is properly designed. To this end is crucial to know the mechanisms and details by which the airflow in the cavity moves and transports heat from the roof toward the ceiling and vice-versa.

Several authors have studied buoyancy driven flows in cavities motivated by a number of engineering applications. Rectangular cavities ([1], [2], [3], [4], [5], [6]), triangular cavities ([7], [8]) and also cylindrical cavities [9] have received special attentions. The latter geometry has also been applied to study sterilization processes of canned foods [10].

Recently, Basak et al. [8] numerically solved a natural convection model in a triangular cavity employing the penalty finite element technique. The goal was to study the temperature distribution and the heat transfer through the base of a closed triangle that very much resembles a roof with an attic space. Their predictions show that the amount of heat transferred through the base increases with the Rayleigh number, i.e. with the flow speed; they also conclude that the Prandtl number has much less influence on heat transfer than the Rayleigh number.

Hirunlabh et al. [11] analyzed the performance of Roof Solar Collectors (RSC) in several different design configurations; they studied the airflow rate through a channel of constant section located just beneath the RSC and found that the induced flow rate depends on both roof inclination and solar intensity radiation. Nonetheless, they also found that not even those configurations that maximize the air convection=provide sufficient natural ventilation as to satisfy resident's comfort. Ciampi et al. [12] studied a roof configuration similar to the one analyzed by Hirunlabh; they paid particular attention to microventilation, i.e. to roof with small-sized-thickness ducts in which the airflow is laminar. The airflow rate in the channel depends not only on the heat field but also on several other factors like duct geometry, fluid dynamic head losses, etc, and it is estimated through an equation obtained from a simplified one-dimensional flow model. These authors found that microventilation might produce energy savings as large as 30%, this percentage can be improved with larger flow passage sections and larger roof inclination angles.

Asan and Namli [13] numerically analyzed the two-dimensional laminar convection in a closed triangular cavity shaped by an inclined roof and a suspended ceiling. Assuming summer day boundary conditions, they used the stream function-vorticity formulation to solve the equation for different values of the Rayleigh number. These authors concluded that the height-base ratio of the triangle is the parameter that most affects the heat transfer through the base; in fact, as this ratio increases they found that heat transfer decreases.

Oztop et al. [14] solved a very similar problem, i.e. they used the same geometry, boundary conditions and numerical formulation as Asan and Namli, but they also considered a roof with and without eaves. The predictions obtained by Oztop et al. show that heat transfer strongly depends on both the aspect ratio and the length of the overhanging portion of the roof.

The analyses performed in all the works previously mentioned were carried out on closed cavities; the goal of the present work is to assess the influence that natural ventilation of the cavity might have on the amount of heat conducted through the ceiling toward the interior of the house. For that purpose we will employ geometries similar to those used by Asan and Namli —which are also similar to the roof geometries analyzed by Oztop et al.— but we will also consider openings located on the lateral walls supporting the roof. Thus, natural ventilation will occur driven by buoyancy forces originated in the temperature difference that exist between the roof and the ceiling. The temperature gap will be extreme on summer days when the roof is exposed to solar radiation and more energy will be consumed by the air conditioning system to keep the interior comfortable.

In the next section we present the main features of the model under analysis, i.e. the geometry of the cavity, the governing equation, and the appropriate boundary conditions to be used when the ceiling is insulated and when it is not. In a short third section we summarize the numerical technique employed and we validate the code by comparing our numerical predictions with results already published. In section fourth we present the results obtained while the last section is devoted to conclusions.

2. The model

Figure 1 sketches the shape of the domain where the governing equations have to be solved; the roof, the ceiling and the lateral walls with openings delimit the domain. The adopted length of the openings was 30 cm, which is the standard thickness of an exterior wall made out of bricks, and the adopted height was 15 cm; the parameter Am is the average height of the cavity, i.e. the distance between the roof and the ceiling at the center of the domain length. The air in the cavity is set into motion driven by buoyancy forces; i.e. the density gradients originated in the temperature difference that exists between the roof and the ceiling induces the air motion. The phenomenon just described is known as natural convection; this type of flow is usually solved with the aid of the so-called Boussinesq approximation that considers the density differences small enough to be neglected everywhere, except for the term where the density affects the gravity force; in that case the density is supposed to linearly change with temperature. In addition to incompressibility, which is already implied in the Boussinesq

approximation, we will assume steady-state laminar flow regime and negligible thermal radiation effects as well as viscous dissipation [15].

2.1. Governing equations

The set of dimensionless governing equations for natural convection flow in a 2-D cavity is given by the equation of continuity (1), the x- and y- components of the momentum equation (2), (3), and the thermal energy equation (4)

$$\frac{\partial u}{\partial x}+\frac{\partial v}{\partial y}=0 \tag{1}$$

$$u\frac{\partial u}{\partial x}+v\frac{\partial u}{\partial y}=-\frac{\partial p}{\partial x}+\left(\frac{1}{\mathrm{Re}}\right)\left(\frac{\partial^2 u}{\partial x^2}+\frac{\partial^2 u}{\partial y^2}\right) \tag{2}$$

$$u\frac{\partial v}{\partial x}+v\frac{\partial v}{\partial y}=-\frac{\partial p}{\partial y}+\theta+\left(\frac{1}{\mathrm{Re}}\right)\left(\frac{\partial^2 v}{\partial x^2}+\frac{\partial^2 v}{\partial y^2}\right) \tag{3}$$

$$u\frac{\partial \theta}{\partial x}+v\frac{\partial \theta}{\partial y}=\left(\frac{1}{\mathrm{Re}\,\mathrm{Pr}}\right)\left(\frac{\partial^2 \theta}{\partial x^2}+\frac{\partial^2 \theta}{\partial y^2}\right) \tag{4}$$

In equations (1)-(4) $Re= \rho U_C L/\mu$ and $Pr= \nu/\alpha$ are the Reynolds and Prandtl numbers respectively; the employed values of the physical properties of the air (density, viscosities, thermal diffusivity and thermal expansion coefficient) are obtained at the mean temperature between the roof and the ceiling ($(Tr+Tc)/2$). Lengths are measured in terms of the ceiling length (L), temperatures are measured in terms of the temperature difference between the roof and the ceiling (Tr-Tc) and velocities are measured in terms of the characteristic velocity (U_C) which is here defined as $(\beta\, L(Tr-Tc)\, g)^{1/2}$; being β and g the thermal expansion coefficient and the gravity constant, respectively.

When a thermal insulating layer is located between the ceiling and the cavity, as is shown on the left of figure 1, the thermal energy equation for the 2-D heat transfer in the solid (5) must be added to the equation set shown above.

$$0=\left(\frac{\partial^2 \theta}{\partial x^2}+\frac{\partial^2 \theta}{\partial y^2}\right) \tag{5}$$

2.2. Boundary conditions

The boundary conditions employed for both momentum and energy equations are summarized in figure 1. When an insulated ceiling is considered, the appropriate additional boundary condition to be imposed is shown in a shaded rectangle appearing at the bottom left side of figure 1. As this figure shows, on solid walls the non-slip condition is imposed. At the openings we assume zero traction vector ($\boldsymbol{T.n}=0$), the atmospheric pressure is arbitrarily set equal to zero and we neglect heat conduction ($\partial\theta/\partial n=0$). At the air entrance, in addition to the air temperature, the y- and x-components of the velocity are imposed; they are set as zero and constant (($\partial u/\partial y=0$), respectively.

The temperature of both the roof and the ceiling is constant (Tr and Tc) and their dimensionless values are one and zero, respectively. The lateral walls are supposed adiabatic, thus ($\partial\theta/\partial n=0$). Finally, if an insulating layer is set on the ceiling, the flow of thermal energy between the air and the

material must be continuous; thus, if b is the dimensionless thickness of the insulating layer, at y = b the following relation applies

$$K_I \frac{\partial \theta}{\partial x} = K_A \frac{\partial \theta}{\partial y} \tag{6}$$

where $\boldsymbol{K_I}$ and $\boldsymbol{K_A}$ are the coefficients of thermal conductivity of the insulating material and the air, respectively.

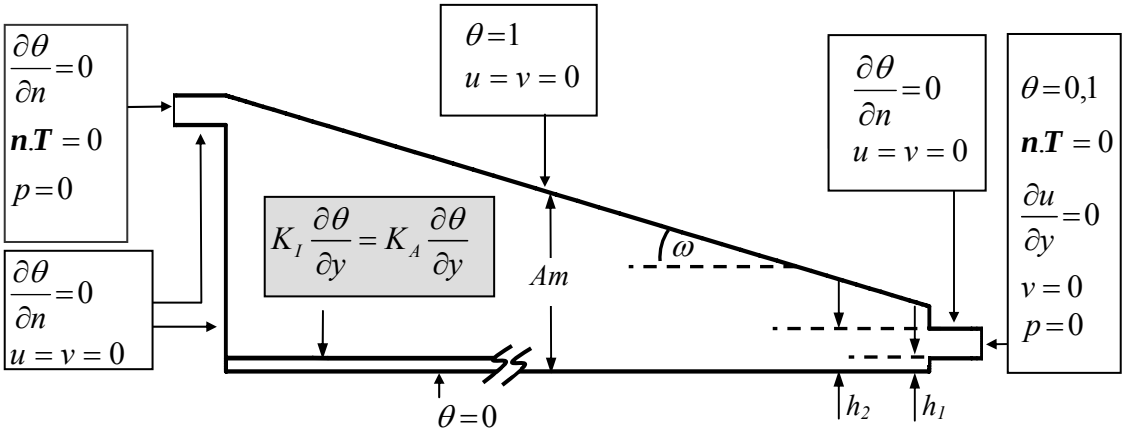

Figure 1. Schematic view of the cavity analyzed and boundary conditions imposed. The left half of the figure shows an insulated ceiling while the right half shows a ceiling without insulation.

3. Numerical technique

The highly nonlinear and strongly coupled system of governing equations can only be solved by numerical means; for that purpose we employed the Galerkin/finite element approach. This is a combination of the Galerkin's weighted residual method with trial functions having support on a few elements into which the flow domain is subdivided. In this work we used the so-called mixed interpolation technique on quadrilaterals; i.e. we adopted biquadratic trial functions for the expansion of velocities and temperature, while bilinear basis functions were employed for pressure. The resulting set of nonlinear algebraic equations was solved with the aid of isoparametric mapping and Newton iteration. The solution path along Reynolds numbers was traced using zero order continuation; i.e. the results obtained for a previous Reynolds value were used as a first guess to start the new Newton iteration for a Reynolds value not too much different from the preceding one.

The numerical algorithm was implemented in Matlab 6.0 on a Window XP platform and the computing time needed to solve 13000 degrees of freedom in a PC Pentium IV of 3.0 Ghz and 1.0 Gb of Ram was about 20 minutes.

4. Results

4.1. Validation of the model.

In order to validate our model we made comparisons with the results presented by Barak et al. [8] and by Haese and Teubner [16]; these comparisons are summarized in figure 2.

Figure 2(a) portrays the isotherms that result in a closed triangular cavity due to air natural convection; the shape of the triangular cavity is just the lower half of a square divided along its diagonal. The horizontal wall, which coincides with the abscissa, is at $\theta = 1$ while the inclined wall is at $\theta = 0$ and the vertical wall is adiabatic. Figure 2(b) shows the temperature variation along the

vertical wall when *Pr = 0.71* and *Re = 31.6*; clearly the predictions of our model completely agree with those obtained by the authors just mentioned.

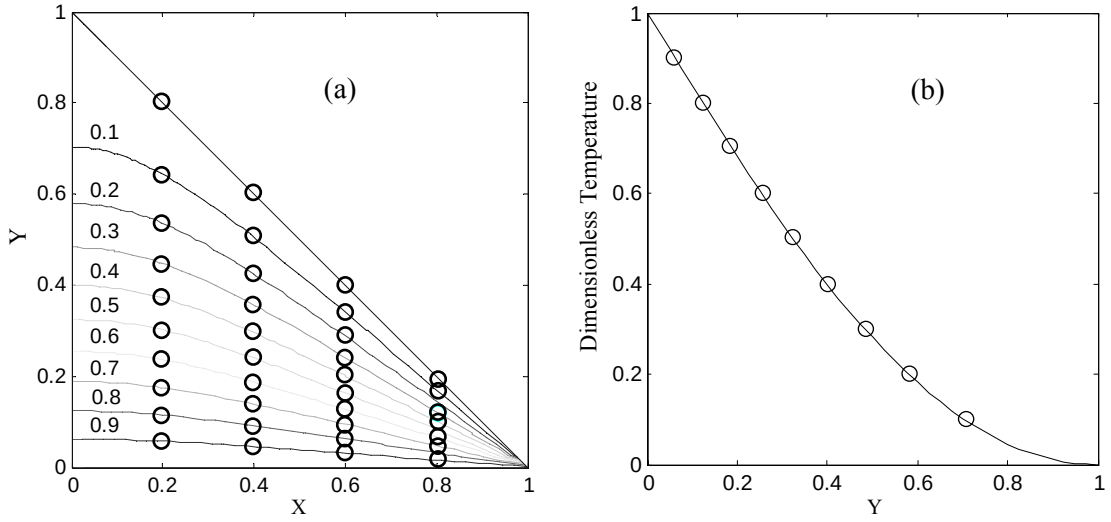

Figure 2. Comparison of the predictions of the present work (full lines) with those obtained by Basak et al. [8] and Haese and Teubner [16] indicated with circles. (a): isotherms in a cavity with a hot horizontal wall, a cold inclined wall and an adiabatic vertical wall. (b): Temperature along the adiabatic vertical wall.

The results to be presented in the following sections were obtained assuming flow motions in laminar regime. Though the natural convection of air in cavities can reach turbulent regimes, particularly for large cavities and strong temperature gradients, analyses assuming laminar conditions are commonly employed to infer the behavior at larger *Re* ([8], [12], [13]).

4.2. A cavity without insulation.

Figure 3(a) compares the amount of heat transferred through the ceiling when air flows across the cavity, and when the openings are closed producing just an inner circulation. The amount of heat transferred is evaluated by computing the average Nusselt number as follows (see [8])

$$Nu = \left(\frac{1}{l}\right)\int_0^l \left.\frac{\partial\theta}{\partial y}\right|_{y=0} dx\,, \tag{7}$$

where *l* is the dimensionless ceiling length, which in our case is just one.

The results shown in figure 3 pertain to a cavity with *Am /L* = 0.22 and a roof with an inclination angle of 15º; they indicate that both open a closed cavities transfer almost the same amount of heat at low values of *Re*, that is so because the air motion is slow and the heat transfer process is dominated by conduction. However, as the *Re* increases both systems behave completely different; while the Nusselt number increases slowly for a closed cavity, it diminishes rather fast for an open cavity. Figure 3(a) shows that the flow rate through the openings increases noticeably with *Re* and most of the heat introduced into the cavity is removed by convection. The consequence is that the two curves depart from each other indicating that a ventilated cavity becomes more convenient as *Re* increases.

Figure 3(b) shows the reduction in the amount of energy that gets across the ceiling when a closed cavity is substituted by a ventilated one. That reduction increases with *Re* and exceeds 50% when *Re* is about 2600.

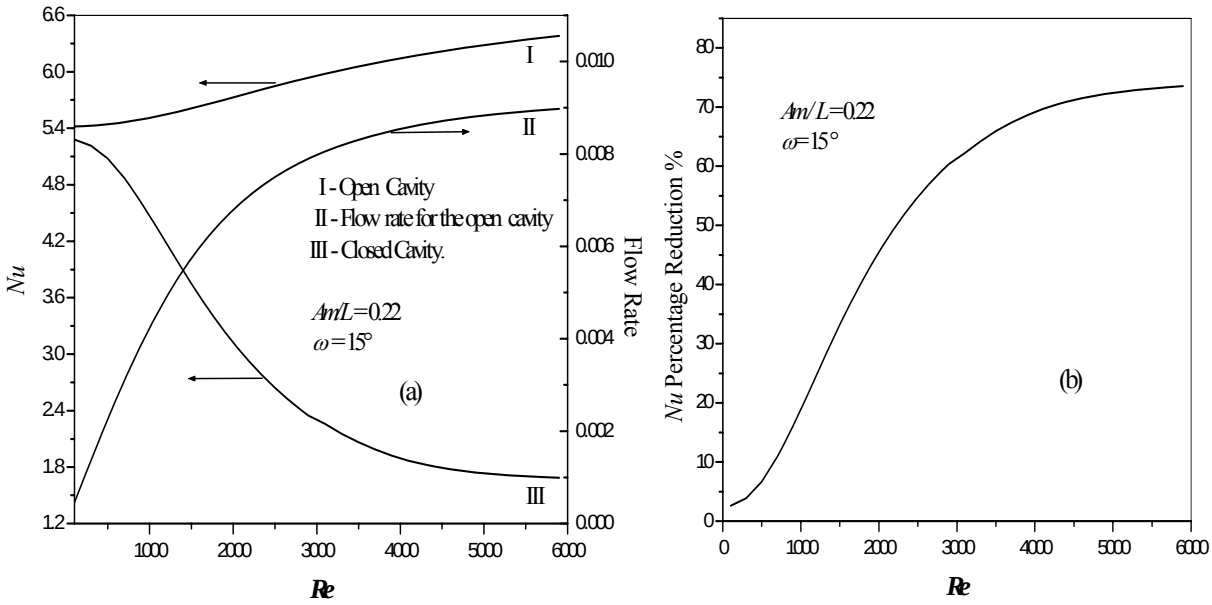

Figure 3. Comparison of the amount of heat transferred through the ceiling for open and closed cavities. (a): Average Nusselt and dimensionless flow rate versus *Re*. (b): Nusselt percentage reduction versus *Re* when an open cavity substitutes a closed one.

In Figure 3(a) the dimensionless flow rate per unit length of the opening is given by

$$q = \int_{h1}^{h2} \mathbf{v}.\mathbf{n}\, dy \tag{8}$$

being $\mathbf{v}$ the dimensionless velocity vector, $\mathbf{n}$ the unit vector normal to the flow passage and h_2-h_1=h (see figure 1) the dimensionless height of the opening.

4.2.1. Influence of the cavity volume (Am/L). Figure 4 shows how the volume of the cavity affects the amount of heat transferred through the ceiling when the inclination angle of the roof is 15º. No matter if the cavity is open or closed, the average Nu decreases as the volume of the cavity increases —i.e. when the ratio *Am /L* increases. Thus, in figure 4 we observe that the curves of constant *Re* have negative slope. For closed cavities, the curves of constant *Re* move upwards as the Reynolds number increases; this result is expected since the heat transported from the roof toward the ceiling should increase with convection. On the other hand, when the cavities are open, more heat should be taken out of the cavities by convection as the Reynolds number increases; therefore, in this case the curves of constant *Re* move downwards. In addition, the results shown in figure 4 indicate that heat transfer is much more sensitive to the Reynolds number in open cavities than in closed ones.

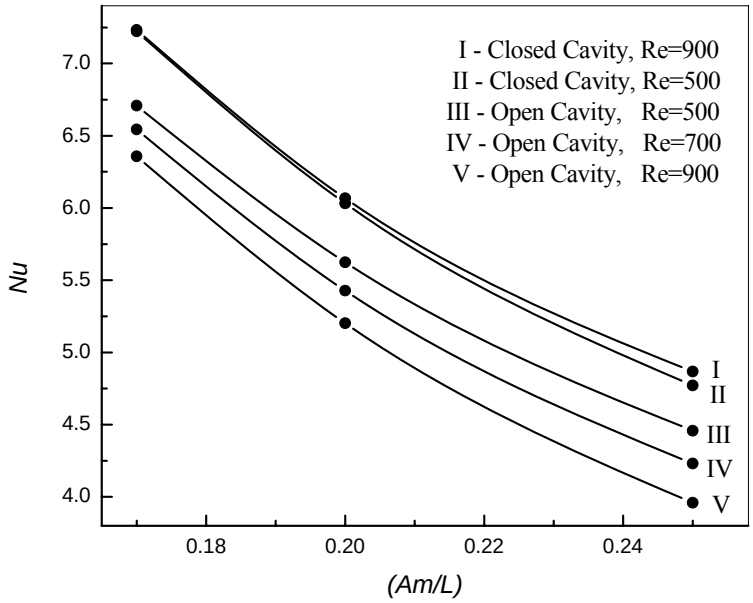

Figure 4: Average Nu versus cavity size (Am/L) for several Reynolds values.

4.2.2. Influence of the roof inclination. Roofs are commonly designed with angles between 10º and 15º, unless the local climate conditions favors the use of larger inclination angles or the space just below the roof will be used for storage purposes. Figure 5 portrays predictions of *Nu* versus *Re* for three different inclination angles; they are 18º, 15º and 10º respectively. These predictions indicate better performances for less inclined roofs; thus, in the range of *Re* explored, the average Nusselt number obtained with an inclination of 10º is approximately 12% smaller than the one obtained with an inclination of 15º. However, in order to favor both drainage and self-cleaning, the inclination angles usually adopted are not too small; for that reason in what follows we use ω = 15º.

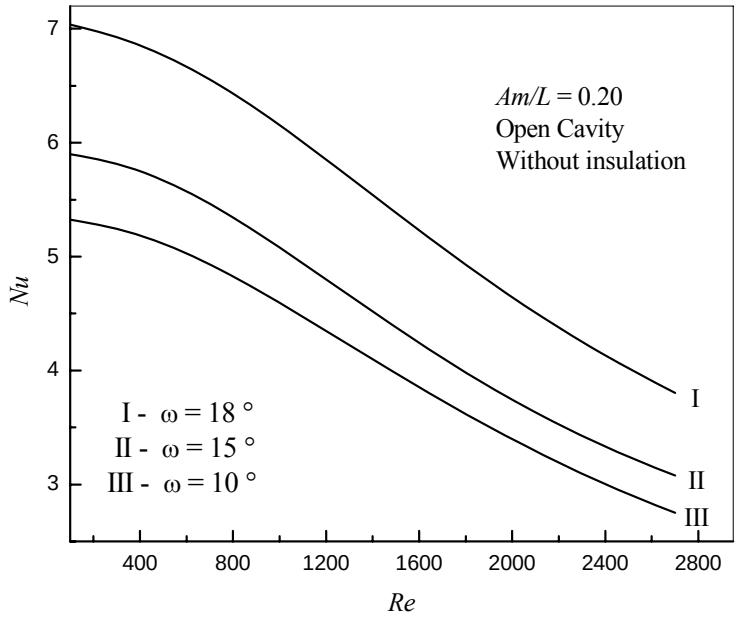

Figure 5. Influence of the inclination on the average Nu for an open cavity without insulation.

4.3. A cavity with an insulated ceiling.

We already pointed out that *Am* is the average distance between the roof and the ceiling (see figure 1); therefore the value of the Am / *L* does not change when a layer of certain insulating material is set on the ceiling as is shown on the left side of figure 1. Also, the adopted dimensionless thickness of the layer (b) is 0.02, which amounts to 8cm in thickness when *L* is 4 m.

In figure 6 we summarize the average Nusselt values obtained for a cavity with and without insulation when $Re \leq 6.1\ 10^3$. On the top of figure 6 the curves denoted as (I) and (II) pertain to a closed cavity and depict the results for the non-insulated cavity and the insulated one, respectively. In this case we have considered an insulation material having exactly the same thermal conductivity as the air; therefore, the ratio between K_I and K_A appearing in (8) is just one ($K = K_I / K_A = 1$). Clearly, at very small values of *Re* the curves coincide since the mechanism of heat transfer is exclusively by conduction. As the values of *Re* increase the effect of convection becomes evident and the insulated cavity performs slightly better allowing less heat to be transferred through the ceiling.

The curves denoted as (III), and (IV) correspond to an insulated and a non-insulated open cavity, respectively. The remarkable outcome is that the non-insulated case performs slightly better than the insulated one when the Reynolds number is smaller than 4.0 103. Both curves are coincident at very small values of the Reynolds number; when Re exceeds 5.0 102 they start to separate from each other until they meet again when the Reynolds value is about 4.1 103. Finally, when Re becomes larger than 4.1 103 the two curves change their relative position indicating that at higher Reynolds the use of an insulated ceiling becomes advantageous. This result was expected since the heat transported toward the ceiling by convection must increase with Re; in addition, this behavior should be enhanced significantly when air flow in the cavity is turbulent.

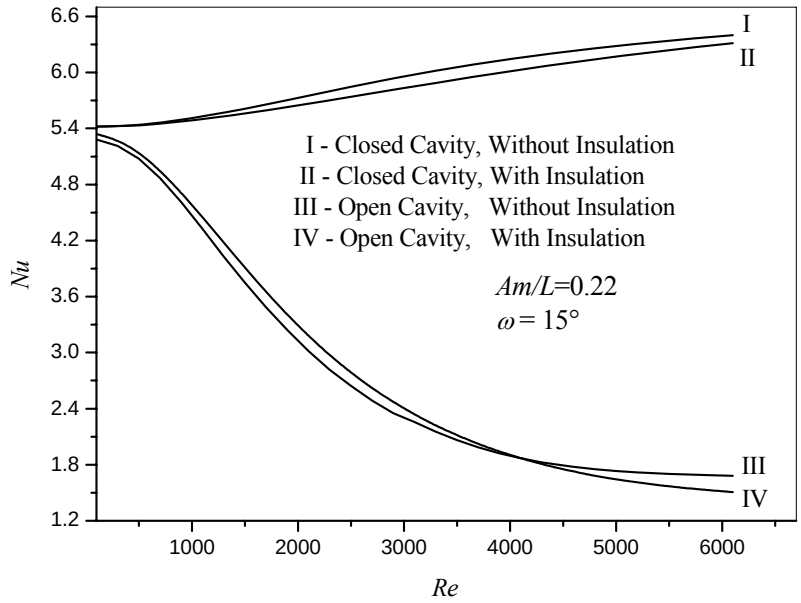

Figure 6. Effect on the average Nu of an insulating layer located on the ceiling of both closed and open cavities.

Figure 6 portrays some interesting results when an open cavity is considered; one of them is that at relatively low values of the Reynolds number, the heat transfer through the ceiling strongly decreases as the air flow rate across the cavity increases, i.e. as the *Re* increases. Actually, when *Re* is about $6.0\ 10^3$ the heat transfer is just 28% of the amount of heat transferred at *Re* smaller than 200. However, if *Re* is further increased the curve of *Nu* becomes almost horizontal indicating that no additional benefits are gained as long as the flow keeps its laminar regime. It is not known the exact value of the Rayleigh number at which turbulent regime appears in this type of cavity, but it is believed that it

might happens when the values are between 10^7 and 10^8 [17]. These values occur when the Reynolds number we use in this work is in the range: $3.7\ 10^3$ - $1.2\ 10^4$.

Another result that must be noticed is the small effect produced by the insulating layer located on the ceiling; the reason for this behavior is a consequence of both temperature and flow fields in the cavity. The temperature field shows that the air inside the cavity is rather stratified, being the warmer layers located near the roof and the cooler ones near the ceiling. Though the warmer layers move at considerable speeds toward the exit openings, the cooler layers are almost stagnant; therefore the heat in this region is mostly transported by conduction and the insulating layer produces just a small reduction in the heat transported.

5. Conclusion

In this work we have studied the influence of a ventilated attic on the heat transferred from the roof and through the ceiling, toward the interior of a building of a family house. We numerically solved the complete set of governing equations that couples flow and heat transfer in natural convection. For that purpose, and in addition to the usual Boussinesq approximation, we made two important assumptions: namely, the air flow is in laminar regime and radiation has negligible effect on heat transfer. Under these assumptions we found that on hot summer days, an attic with suitable openings can significantly reduce heat transfer and produce considerable energy savings in air conditioning.

If one assumes that an appropriate radiant barrier is employed, the results obtained should also be valid regardless of how important the radiation transfer might be. Nonetheless, in future analyses we will consider the influence of radiation and we will also explore the turbulent regime —which might occur if the roof temperature is high enough— where the heat transfer by convection should be more important and the employment of insulating layers must be necessary to preserve significant energy savings.

Acknowledgements

This work was supported by grants in aid from Universidad Nacional del Litoral, Concejo Nacional de Investigaciones Científicas y Técnicas (CONICET) and Agencia Nacional de Promoción Científica y Tecnológica of Argentina.

References

[1] Nawaf, S H 2007. Conjugate natural convection in a vertical porous layer sandwiched by finite thickness walls. *International Journal of Heat and Mass Transfer*. **34** 210–16.

[2] Das M K, Reddy K S 2006. Conjugate natural convection heat transfer in an inclined square cavity containing a conducting block. *International Journal of Heat and Mass Transfer.* **49** 4987–5000.

[3] Muftuoglu A, Bilgen E 2008. Heat transfer in inclined rectangular receivers for concentrated solar radiation. *International Journal of Heat and Mass Transfer.* **35** 551-56.

[4] Bilgen E, Yedder R B. 2007. Natural convection in enclosure with heating and cooling by sinusoidal temperature profiles on one side. *International Journal of Heat and Mass Transfer.* **50** 139–50.

[5] Altac Z, Kurtul Ö 2007. Natural convection in tilted rectangular enclosures with a vertically situated hot plate inside. *Appl. Ther. Eng*. **27** 1832– 40.

[6] Lamsaadi M, Naïmi M, Hasnaoui M 2006. Natural convection heat transfer in shallow horizontal rectangular enclosures uniformly heated from the side and filled with non-Newtonian power law fluids. *Energy Conversion and Management*. **47** 2535– 51.

[7] Varol Y, Oztop H. F, Tuncay Yilmaz. 2007. Natural convection in triangular enclosures with protruding isothermal heater. *Int. J. of Heat and Mass Transf*. **50** 2451–62.

[8] Basak, T, Roy, S, Thirumalesha, Ch 2007. Finite element analysis of natural convection in triangular enclosure: Effects of various thermal boundary conditions. *Chemical Engineering Science*. **62** 2623– 40.

[9] Cesinia G, Paroncinia M, Cortellab G, Manzanb M 1999. Natural convection from a horizontal cylinder in a rectangular cavity. *Int. J. of Heat and Mass Transf*. **42** 1801-11.
[10] Kannan A, Gourisankar Sandaka PCh 2008. Heat transfer analysis of canned food sterilization in a still retort. *Journal of Food Engineering*. **88** 213-28.
[11] Hirunlabh, J, Wachirapuwadon, S, Pratinthong, N, Khedari, J 2001. New configurations of a roof solar collector maximizing natural ventilation. *Building and Environment.* **36** 383– 91.
[12] Ciampi, M, Leccese, F, Tuoni, G 2005. Energy analysis of ventilated and microventilated roofs. *Solar Energy*. **79** 183–92.
[13] Asan, H, Namli, L 2000. Laminar natural convection in a pitched roof of triangular cross-section: summer day boundary conditions. *Energy and Buildings*. **33** 69-73.
[14] Oztop H F, Varol Y, Koca A 2007. Laminar natural convection heat transfer in a shed roof with or without eave for summer season. *Applied Thermal Engineering*. **27** 2252–2265.
[15] Jaluria, Y 1980. *Natural Convection. Heat and Mass Transfer*. Vol V, ed D B Spalding (Imperial College of Science and Technology, London, England: Pergamon Press). P 326.
[16] Haese, P M, Teubner, M D 2002. Heat exchange in an attic space. *International Journal of Heat and Mass Transfer.* **45**(5) 4925– 36.
[17] Papanicolaou, E and Belessiotis, V 2005. Doubble-diffusive natural convection in an asymmetric trapezoidal enclosure: unsteady behaviour in the laminar and the turbulent-flow regime. *International Journal of Heat and Mass Transfer*. **48** 191-209.